

## Geochemical Characteristics of Sedimentary Manganese Deposit of Binkılıç, Trache Basin, Turkey

Ali Haydar Gültekin\* and Nurgul Balci

Department of Geological Engineering, Istanbul Technical University, Ayazaga Campus, 34469 Maslak, Istanbul, Turkey

### Abstract

The Binkılıç manganese deposit, occurring in the Congeria and Fish Series of the Oligocene in Thrace Basin, is associated with relatively rapid marine transgressions and regressions across older basement rock and is called as shallow-marine basin-margin deposit. The geochemical characteristics of the deposit were examined by means of major oxide, trace and rare elements (REE) contents and the origin of mineralization was discussed. The deposit contains lower Mn / Fe ratios than those of hydrothermal and sedimentary exhalative deposits. The concentrations of Ba, Co, Sr, Cu, Zn and Ni are closely related to the increase of manganese content and indicate the element's nature in various manganese minerals. According to trace element spider diagram normalized to shale composite NA, the ore is clearly enriched in Sr, Ni while distinctly depleted in Rb. The chemical analysis results indicated that total REE contents of the samples are relatively low and the ratio of  $\Sigma$ LREE/ $\Sigma$ HREE shows a primary enrichment for LREE that has occurred during the Mn oxidation process. The increase in total LREE is mainly associated with the amount of terrigenous material that was transported in the depositional environment. The chondrite-normalized REE patterns are remarkably similar, yielding HREE-depleted curves with a small negative Ce and middle positive Eu anomalies and reflect their same origin of ore source. The Ce values and Ce/Ce\* ratios show that the Binkılıç deposit is mainly associated with the marine basin and the ore is formed in both anoxic and oxic conditions. The major oxide, trace element and REE assessments indicated that the Binkılıç Mn deposit occurred as a diagenetic type of Mn deposit with terrigenous material addition, but some manganese oxides are related to the upwelling of reducing waters containing abundant organic matter and dissolved Mn to the shallow-marine areas.

**Keywords:** Manganese ore; Trace element; Rare earth element; Environment; Basin margin

### Introduction

The resources of sedimentary and hydrothermal Mn-deposits are wide spread in Turkey, and the total reserves are approximately 50 Mt [1,2]. The manganese deposits of the Thrace basin, occurring at the transition from limestone deposition below to clastic deposition above, are the most important sedimentary type deposits of Turkey (Figure 1). These Oligocene deposits are coeval and intermittently connected with the other sedimentary manganese deposits of the paratethys, such as Nikopol in Ukraine and Chiatura in Georgia. All the deposits, fatter to the east in the Paratethys, are stratiform and extend within predominantly clastic series [3-5].

Mn deposits, found in various part of Turkey reflect the various tectonic settings [1,2,6-9]. These deposits were grouped in five types based on their mineralogy, composition and tectonic settings: (1) sedimentary (hydrogenous), (2) volcanic-sedimentary, (3) hydrothermal, (5) hydrothermal modified, and (5) diagenetic. The percentage distribution of reserves of these genetic types indicates that sedimentary deposits comprises of a significant majority [1,2]. Sedimentary Mn deposits are mostly precipitated in a shallow subbasin and contain amorphous Fe and Mn-oxides with a Mn/Fe ratio of ca. 1. They are characterized by the high Ni and Cu concentrations, low Mn-Si content and weakly negative Ce anomalies. Such main deposits are primarily hosted by carbonate rocks, mudrock, and chert-mudstone-limestone [2].

Volcanic-sedimentary Mn deposits contain the submarina hydrothermal affects and are mostly represented by the negative Ce anomaly. The hydrothermal Mn deposits in Turkey are mainly volcanic rock-hosted Fe-Mn oxide ores. They occur as open-space fillings in faults, fractures and breccias in the andesites and dasites of the island-arc and directly precipitated from low-temperature hydrothermal solution [9]. Some hydrothermal Mn deposits are hosted by radiolarite cherts, widely in epiophiolites of Paleotethys and show high Mn-Si and low

Al-Fe contents. Diagenetic Mn deposits, other types occur as nodules and are precipitated from hydrothermal solution or pore waters within altered sediments [10]. Fe contents of these deposit is higher and Si content is lower than that of those in radiolarite chert.

Manganese deposits of Turkey have been a subject of various researches mostly focusing on hydrothermal Mn deposits located in the NE and SW of Turkey. At Thrace Basin, sedimentary manganese deposits lie in the Congeria and Fish Series of the Oligocene and contain abundant manganese ore tonnage. The Çakıllı, Binkılıç and Çatalca deposits are main manganese mines of the basin (Figure 1a).

The geology and stratigraphy of the Mn oxide-bearing sedimentary formations of the Thrace basin are first described by Akartuna [11]. According to Bora [12], the deposits are stratiform but apparently discontinuous along strike and display evidence of significant diagenetic alteration of primary carbonate minerals. Most extensive data on the metallogenic history and exploration potential of the district can be found in Uzkut [13]. In the last few decades, further investigations were carried out on the manganese ores of the Thrace-Binkılıç mine. Öztürk and Frakes [5] were described the sedimentation and diagenesis of Binkılıç Mn deposits; they measure the ore thickness of about 5 m, contain marine fossils. The close association of Mn-oxides with hydrogenous conditions along paleoshorelines was described in detail by Gültekin [8].

\*Corresponding author: Ali Haydar Gültekin, Department of Geological Engineering, Istanbul Technical University, Ayazaga Campus, 34469 Maslak, Istanbul, Turkey, Tel: +90-212-285-6119; E-mail: [ahgultekin@hotmail.com](mailto:ahgultekin@hotmail.com)

Received March 22, 2018; Accepted April 09, 2018; Published April 16, 2018

Citation: Gültekin AH, Balci N (2018) Geochemical Characteristics of Sedimentary Manganese Deposit of Binkılıç, Trache Basin, Turkey. J Geol Geophys 7: 336. doi: 10.4172/2381-8719.1000336

Copyright: © 2018 Gültekin AH, et al. This is an open-access article distributed under the terms of the Creative Commons Attribution License, which permits unrestricted use, distribution, and reproduction in any medium, provided the original author and source are credited.

Manganese mines of the Binkılıç area are located about 47 km NW of the city of Istanbul on the Thrace Peninsula in NW Turkey (Figures 1a-1c). The Binkılıç area is roughly 30 km (west to east) and 10 km (north to south) in size and encompasses one mine which was active until 1987 and two idle mines as well as several large prospects. The mine is the most important manganese mineralization of the Thrace basin and consists of battery-grade Mn oxides. This deposit was the main Mn source of Turkey during the period of 1970-2000 and furnished nearly 200 000 tons of manganese ore during the 10- year period of 1990-2000.

Despite the previous studies, a comprehensive geochemical characteristic of the deposits are still lacking. The purpose of this study is to present the main geochemical characteristics of sedimentary Mn deposit in Binkılıç area, and discuss the manganese sources and formation conditions of the ore. Therefore, assessment of major and trace element contents of Mn deposits would be useful for elucidating not only deposition conditions of the ore but also Mn sources in detail. Overall, the results presented in this study may provide a useful guide for the exploration of similar ore deposits in the region.

## Geologic Background of Manganese Deposit

The Thrace basin is a Tertiary collisional-collapse type basin which bounded to the south and west by older massifs such as Rhodope, Biga, Kapıdağ and Samanlıdağ [5]. The Mn deposit district at Binkılıç is placed adjacent to the Stranjha Massif in the Thrace Basin. The Massif contains low grade metamorphic cover rocks of Mesozoic age, so called as crystalline basement. This crystalline basement is also the oldest lithostratigraphic unit in the Binkılıç area and includes an iron-rich Mn deposit up to a few meters thick, namely Kestanepınar Mn deposit [11]. The intensively folded metamorphic rocks of the basement intruded by younger granite. Other units exposing in the region are Tertiary sedimentary rocks of Thrace basin. The basin was influenced by tectonism as a whole, but structural deformation of Thrace basin strata is strong only near the southern margin [12].

Tertiary sedimentary succession is very thick in the center of the basin but thins towards the northern margin. The first accumulation began in the early Eocene, as basal conglomerate and near shore sands related to a transgression (Figure 2). These early Eocene rocks lie directly upon the metamorphic basement. Later Eocene deposition in Thrace basin, especially near the margin, is reflected by fossil-rich micritic limestones and is separated by a marked angular unconformity from the metamorphic basement. The Eocene conglomerates and sandstones with claystone interlayer were made up of the material from the basement rocks that were worked by longshore currents and waves. This unit is locally a few ten meters or at least several centimeters thick and is characterized by a fining-upward grain-size. The micritic limestones are represented by sedimentation associated with transgressive marine conditions that returned to the district during Lutetian and are mostly overlain by a marine sequence of Oligocene limestones [8].

The Oligocene sequence, separated by an unconformity from Eocene, is divided into two units, the Congerian Series below and the Fish Series above (Figures 1 and 2). Its thickness varies from 50 to 150 meters. The lower part of the Oligocene, about 80 m meter thick, is marked by a transition containing an abundance of the pelecypod genus *Congeria*, gastropods, foraminifera and ostracods [5,14]. The Congerian Series consists of conglomerate in the southeast and grades to limestone to the northwest. This Series was deposited under shallow water conditions, possibly a lagoon environment linked with the open sea because of absence of chemical sediments such as evaporate. The

upper part (Fish series), 60-70 meters thick, is composed of silty claystones, organic material-rich marl and finely laminated sandstone. The Fish Series, also called as Karton series reflect various facies of a delta. Near the base of a 20-m-thick section of the Congerian and Fish Series at Binkılıç, the first significant occurrences of manganese are observed. According to the results of exploration drilling in the Binkılıç mine, the average thickness of Mn oxide ore is approximately one meter.

The Oligocene sediments are unconformably overlain by Miocene series that are mainly composed of sandstone and marl. This sequence is directly taken the place above the main ore level in the east and like Oligocene sequence, is essentially undeformed, although Eocene and Pre-Eocene fault block movements have occurred in the region. Pliocene sediments at Binkılıç are composed of gray-yellow weakly cemented conglomerate, sandstone, sand and clay that is continental in origin and irregularly blanket the northern margin of the basin. The clay, sand and gravel sequences of Quaternary age are the youngest lithostratigraphic unit in the Binkılıç district.

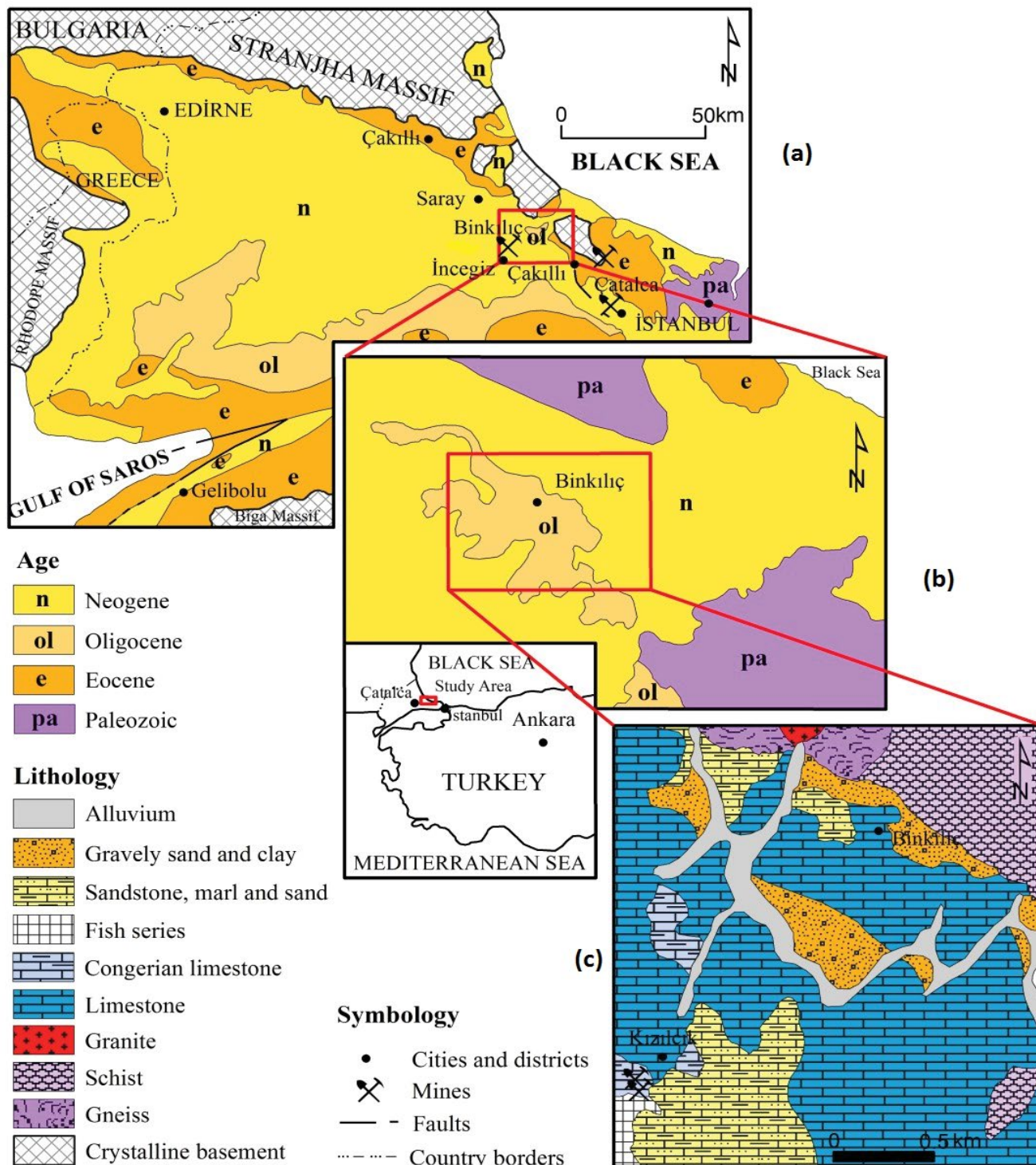
## Materials and Methods

Sample material was taken from open-pit locations for geochemical study throughout district. Total 21 systematic samples (18 ore samples and 3 wallrock samples) were collected from the Binkılıç Mn deposit. Approximately 1-2 kg material was sampled in each location. 500 gr chips for each sample were carefully selected, washed with distilled water at room temperature, and then dried at 105°C. In the laboratory, massive and hard materials were broken into small chips with a jaw breaker. Then, the chip samples were ground to less than 200 mesh fine powders with an agate mill. A 200 g of split was used for geochemical analyses. The sample powders were analyzed at ACME Laboratories. Major oxide and trace element contents were determined with ICP-ES and REE's were analyzed with ICP-MS method. The analytical results are presented in (Tables 1-3).

## Characteristics of the Ore Body

The characteristics of the ore body are discussed here within a framework of structural types, that is, oolitic/pisolitic ore, detritus-rich ore, massive manganese and broken pisolitic ore. The Oolitic/pisolitic ore is generally high grade, hard ore including gray clay balls or calcite infillings, and spicule and voids representing dissolved pisoliths. This type ore is sedimentary oxidic ore that account for approximately 95% of the total reserves of the deposit and consists dominantly of pyrolusite and manganite in replacement structures and as a cement [5,8]. The external bonding surfaces of oolites and pisoliths are typically smooth, relatively dense and rare comprise tightly interlocking Mn oxide microcrystals. The detritus-rich ore consists of fine-to medium-grained clastic material weakly cemented by Mn oxides. This type ore mostly developed in the lower and upper levels of manganese oxide strata. The clastic material mostly composed of quartz, feldspar, and clay mineral in minor amounts. The massive ore contain very fine beds and consists mostly of psilomelane, and manganite but other Mn oxides occur as well. It is generally a high grade, sometimes soft ore that include yellowish clay balls in minor amount. The broken pisolitic ore contain mainly pyrolusite, psilomelane and cryptomelane but also traces of lepidochrosite. In the ore level, the broken pisoliths, about 1 cm diameter, occur together with shell hash of *Congeria* and make up about 30% of the unsorted sediments [5].

The mineralogy of the deposit, in general is relatively simple, with the main ore minerals being pyrolusite, psilomelane, manganite, cryptomelane which constitute more than 90% of the total ore



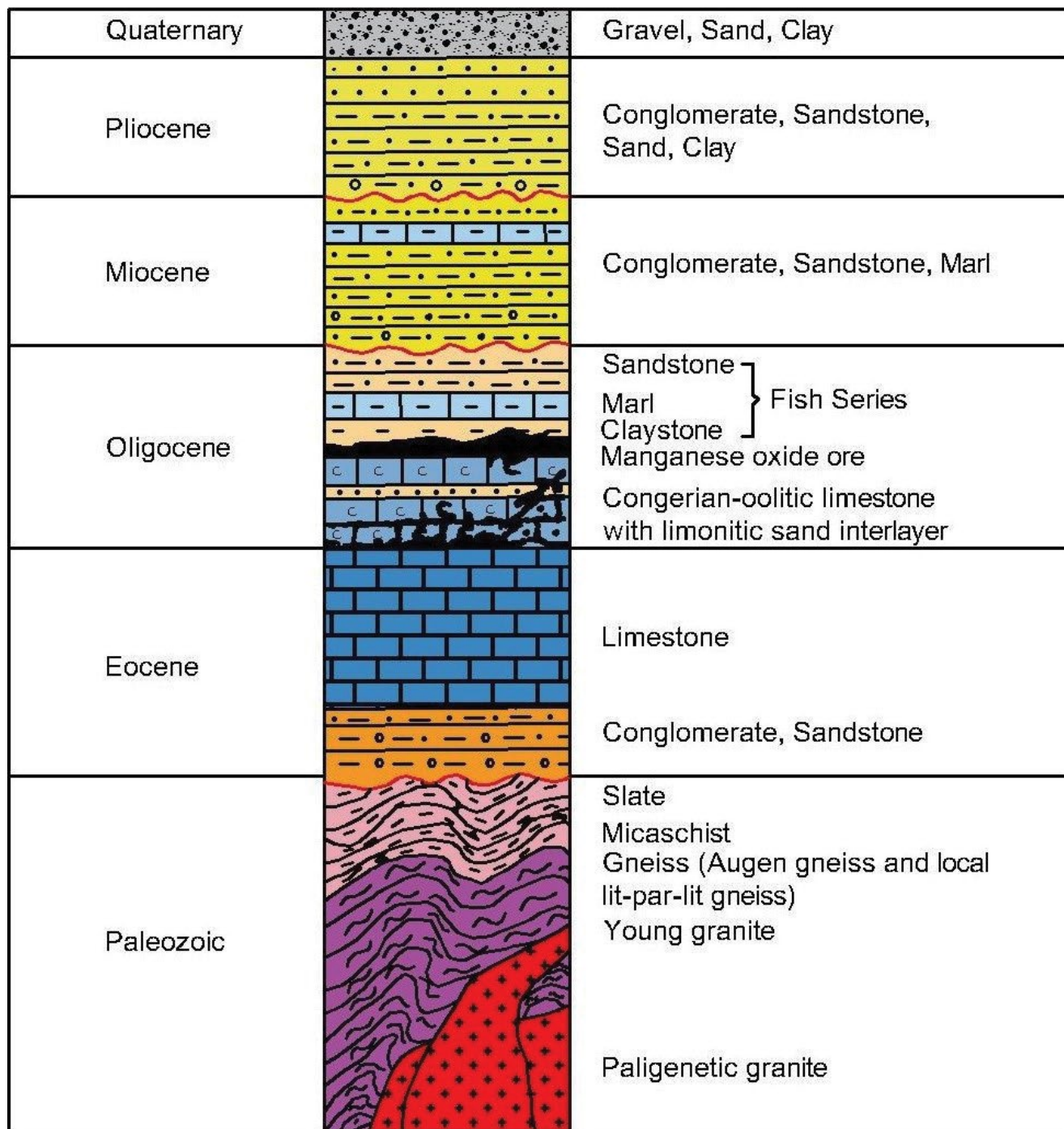


Figure 2: Stratigraphic section of the Binkılıç district (Gültekin , 1998; Oztürk and Frakes, 1995).

assemblage. Calcite, rhodochrosite, kutnahorite, manganocalcite, quartz, feldspar, limonite, goethite, and clay minerals are other members of the Binkılıç mineral assemblage [8].

### Geochemical Characteristics of the Binkılıç Manganese Deposit

#### Major and trace element geochemistry

Major and trace element contents of the samples taken from

the Binkılıç Mn deposit are presented in Table 1 and 2, respectively. According to the ore types, the highest Mn values are determined in the massive ore (41,17% Mn) and Oolitic/pisolitic ore (38,56% Mn). The detritus-rich ore contains low values because of high content of clastic material. This type of ore has an average of 10,95%Mn. In the Binkılıç oolitic/pisolitic ore, iron and manganese are characteristically fractionated, producing high Mn/ Fe ratios. Similar character is also seen in massive ore. Both types have a varying Fe / Mn ratio between

Samples	SiO <sub>2</sub>	Al <sub>2</sub> O <sub>3</sub>	Fe <sub>2</sub> O <sub>3</sub>	MgO	CaO	Na <sub>2</sub> O	K <sub>2</sub> O	TiO <sub>2</sub>	P <sub>2</sub> O <sub>5</sub>	MnO	LOI	Mn	Fe	Mn/Fe	Al	Ti
BOP03	9,69	1,39	3,69	1,12	16,62	0,43	0,34	0,30	0,97	53,19	12,23	41,17	2,52	16,34	0,74	0,18
BOP04	4,01	3,50	4,00	1,04	17,50	0,50	0,24	0,50	1,10	49,00	11,52	37,92	2,80	13,54	1,86	0,30
BOP05	7,30	1,15	3,97	1,18	16,98	0,20	0,22	0,20	0,60	55,01	12,95	42,58	2,78	15,32	0,72	0,12
BOP06	5,20	5,80	2,77	1,25	8,50	0,41	0,70	1,18	0,45	46,06	26,68	35,72	1,96	18,22	0,61	0,71
BOP08	6,50	5,10	1,05	1,08	14,43	0,13	0,37	0,90	1,05	55,00	14,43	42,57	0,73	58,31	2,72	0,54
BOP09	7,78	0,49	8,10	0,92	16,53	0,40	0,35	0,16	0,96	39,47	24,68	30,54	5,67	5,38	0,16	0,09
BOP10	6,57	2,60	2,65	0,96	21,63	0,36	0,39	0,41	0,78	50,94	12,67	39,42	1,85	21,30	1,38	0,24
BM12	3,93	1,13	2,54	1,33	6,74	0,58	0,17	0,80	0,25	66,05	16,98	51,12	1,78	28,72	0,60	0,56
BM14	5,93	0,98	3,49	1,21	18,82	0,32	0,42	0,17	0,59	53,45	14,61	41,37	2,44	16,95	0,52	0,10
BM15	7,00	2,60	2,90	0,71	22,01	0,86	0,33	1,05	0,95	49,00	12,57	37,92	2,03	18,67	1,38	0,63
BM18	8,17	0,98	2,50	1,31	19,60	0,27	0,18	1,10	0,90	44,30	13,66	34,28	1,75	19,58	0,52	0,66
BD23	10,33	8,05	0,34	0,60	33,90	0,12	0,10	0,96	0,57	6,64	38,75	5,14	0,24	21,42	0,26	0,58
BD25	35,34	16,32	2,50	0,80	19,01	0,90	0,40	1,32	0,25	15,04	7,01	11,64	1,75	6,65	8,18	0,79
BD27	25,07	8,90	8,80	0,65	31,66	0,88	1,10	1,01	0,44	11,01	10,91	8,52	6,16	1,38	4,75	0,61
BD28	11,06	2,20	12,40	1,35	25,93	0,21	0,60	0,70	0,26	23,90	23,37	18,49	8,68	2,13	1,17	0,49
BBP29	9,89	7,02	7,27	0,90	17,98	0,55	0,40	0,90	0,27	17,91	36,81	13,47	5,08	2,65	3,74	0,54
BBP31	8,89	2,32	13,40	1,55	25,68	0,21	0,44	0,30	0,23	24,18	22,79	18,72	9,38	2,00	1,23	0,18
BBP32	5,11	1,10	1,65	1,30	25,99	0,12	0,12	0,28	0,72	35,59	28,01	27,55	1,16	23,75	0,59	0,17
BBP33	9,75	1,12	0,75	1,45	46,43	0,15	0,42	0,21	0,48	18,66	27,57	14,44	0,53	27,24	0,60	0,13
BYK20	11,2	3,43	2,01	0,93	42,6	0,25	0,44	0,35	0,72	3,10	35,56	2,40	1,41	1,70	1,82	0,21
BYK21	5,20	0,70	1,90	1,50	45,75	0,10	0,40	0,20	0,60	15,50	28,41	12,00	1,33	9,17	0,48	0,12
BYK26	10,23	3,40	2,31	0,64	46,60	0,11	0,11	0,30	0,63	6,55	39,32	5,07	1,61	3,15	1,80	0,18
MIN.	3,93	0,40	0,31	0,64	6,74	0,11	0,10	0,16	0,23	3,10	7,01	5,07	0,22	1,38	0,21	0,09
MAX.	35,34	16,32	13,40	1,55	46,60	0,90	1,10	1,32	1,10	66,05	39,32	51,12	9,38	58,31	4,75	0,79
AVE.	9,87	3,39	3,99	1,08	24,59	0,37	0,37	0,60	0,68	33,62	21,43	26,00	2,79	16,76	1,74	0,37

BOP: Oolitic/pisolitic ore, BM: Massive ore, BD: Detritus-rich ore, BBP: Broken pisolitic ore, BYK: Wallrock samples.

Table 1: Major oxide contents of the ore and wallrock samples (%).

Samples	Ba	Co	Cr	Rb	Sr	V	Zr	Cu	Pb	Zn	Ni	Sr/Ba	Co/Zn	Co/Ni
BOP03	2216	149	15	21	1010	30	65	120	53	85	350	0,45	1,75	0,43
BOP04	3106	95	15	35	5760	18	63	98	33	71	36	1,85	1,34	0,26
BOP05	2548	94	13	27	2305	42	66	95	51	65	109	0,90	1,45	0,86
BOP06	2415	90	11	16	1980	40	46	86	50	70	91	0,82	1,29	0,99
BOP08	1450	55	20	19	5980	35	49	120	68	50	140	4,12	1,38	0,39
BOP09	2967	90	14	10	5590	21	73	106	30	80	260	1,88	1,13	0,35
BOP10	2814	96	16	19	4530	33	60	112	56	75	275	1,61	1,28	0,35
BM12	2115	90	12	25	3638	20	48	105	36	68	115	1,72	1,32	0,78
BM14	810	62	17	8	350	65	26	85	40	47	64	0,43	1,32	0,97
BM15	3269	85	18	21	3760	31	57	103	38	60	90	1,15	1,42	0,94
BM18	4251	65	16	24	5608	28	66	110	42	45	66	1,31	1,44	0,98
BD23	4320	72	20	38	5410	25	73	115	40	54	102	1,25	1,33	0,71
BD25	2130	42	4	5	168	10	42	68	27	40	216	0,07	0,62	0,19
BD27	780	64	19	10	379	67	33	83	40	42	64	0,48	1,52	1,00
BD28	985	50	3	5	158	122	17	110	33	29	40	0,16	1,72	1,25
BBP29	1079	83	10	6	280	93	25	20	10	108	90	0,25	2,86	0,92
BBP31	2950	95	15	35	5120	34	45	90	46	78	75	1,74	1,22	1,27
BBP32	607	58	24	12	370	33	52	115	65	43	330	0,61	1,35	0,18
BBP33	1233	45	9	22	996	37	24	70	19	35	102	0,81	1,29	0,44
BYK20	2310	85	14	18	2365	30	60	110	34	70	78	1,02	1,21	1,09
BYK21	450	15	5	8	560	47	32	79	59	34	27	1,24	0,44	0,56
BYK26	386	40	10	13	510	15	65	103	38	55	35	1,32	0,72	1,14
MIN.	450	15	3	5	210	10	24	20	10	29	27	0,43	0,19	0,18
MAX.	4320	149	24	38	5980	122	73	120	68	108	350	4,12	2,86	1,27
AVE.	2125	73,64	13,63	18,0	2664	39,82	49,41	95,59	41,27	60,05	125,2	1,15	1,34	0,73

BOP: Oolitic/pisolitic ore, BM: Massive ore, BD: Detritus-rich ore, BBP: Broken pisolitic ore, BYK: Wallrock samples.

Table 2: Trace element contents of the ore and wallrocks samples.

Samples	La	Ce	Nd	Sm	Eu	Gd	Tb	Dy	Er	Yb	Lu	Y	ΣREE	ΣLREE/ΣHREE	Ce/La	Eu/Sm	Sm/Nd	ΣCe/ΣY	La/Yb	Eu/Eu*	Ce/Ce*	Ce <sub>anom</sub>
BOP03	21,01	24,34	14,11	3,02	2,22	3,15	0,67	0,71	2,05	2,13	0,18	10,42	73,59	7,28	1,16	0,74	0,21	3,35	9,86	0,36	0,61	-0,25
BOP04	26,25	45,01	20,22	5,05	4,09	4,52	0,98	3,99	3,32	3,44	0,41	34,02	117,28	6,04	1,71	0,81	0,25	1,95	7,63	0,31	0,85	-0,08
BOP05	43,33	52,11	27,55	5,59	2,19	5,50	3,40	3,61	3,13	3,23	0,47	43,44	150,11	6,51	1,20	0,39	0,20	1,88	13,41	0,20	0,65	-0,23
BOP06	16,44	26,14	14,02	3,97	3,10	1,98	0,76	3,10	1,82	1,80	0,31	15,15	73,44	7,26	1,59	0,78	0,28	2,56	9,13	0,46	0,75	-0,13
BOP08	39,11	13,12	8,23	1,88	0,86	0,65	1,86	0,56	0,62	0,85	0,02	9,33	67,76	13,85	0,36	0,46	0,23	3,00	46,01	0,62	0,25	-0,73
BOP09	37	34,05	21,02	4,99	3,01	4,22	0,78	2,11	2,32	2,05	0,29	13,31	111,84	8,50	0,92	0,60	0,24	3,07	18,04	0,28	0,52	-0,34
BOP10	12,00	25,07	11,89	2,95	1,78	0,76	0,75	3,01	2,02	1,85	0,28	16,61	62,36	6,19	2,09	0,60	0,25	2,12	6,49	0,66	0,92	-0,02
BM12	16,51	22,32	10,78	2,78	1,88	1,75	0,70	0,72	0,59	0,65	0,09	12,55	58,77	12,06	1,35	0,68	0,26	3,18	25,40	0,46	0,72	-0,18
BM14	10,00	15,60	9,62	2,01	2,00	0,74	0,45	0,72	0,80	0,81	0,02	10,57	47,67	11,08	1,56	1,00	0,21	2,88	12,35	0,85	0,69	-0,14
BM15	12,20	20,02	10,10	3,05	2,04	2,11	0,99	1,88	0,86	0,78	0,03	8,33	54,06	7,13	1,64	0,67	0,30	3,16	15,64	0,41	0,79	-0,11
BM18	15,32	21,43	7,89	3,11	1,87	0,81	1,23	2,00	1,65	1,87	0,03	12,55	55,98	6,54	1,40	0,60	0,39	2,62	8,19	0,63	0,82	-0,15
BD23	16,30	22,67	11,43	3,12	3,20	2,13	0,88	2,01	0,89	0,81	0,21	10,38	63,65	8,18	1,39	1,03	0,27	3,28	20,12	0,51	0,72	-0,17
BD25	5,10	6,22	2,98	0,67	0,32	0,45	0,33	0,40	0,52	0,32	0,03	2,80	17,34	7,45	1,22	0,48	0,22	4,56	15,93	0,76	0,68	-0,22
BD27	8,90	9,91	3,65	0,78	0,74	0,69	0,64	0,65	0,55	0,60	0,15	13,43	27,26	7,31	1,11	0,95	0,21	1,62	14,83	0,86	0,71	-0,24
BD28	5,01	10,01	5,22	1,69	0,69	0,78	0,35	0,68	0,80	0,42	0,09	15,15	25,24	7,25	1,99	0,41	0,32	1,30	11,92	0,53	0,85	-0,04
BBP29	26,60	48,65	23,53	5,48	4,40	3,43	2,33	3,53	3,60	3,38	0,43	40,65	125,36	6,51	1,83	0,80	0,23	1,86	7,87	0,36	0,85	-0,07
BBP31	19,33	32,45	15,32	4,02	3,02	2,97	0,79	3,12	2,98	1,89	0,34	21,32	86,23	6,13	1,68	0,75	0,26	2,21	10,22	0,37	0,82	-0,10
BBP32	9,95	16,01	9,72	1,67	1,65	1,82	0,71	1,73	0,67	0,66	0,05	12,03	44,64	6,91	1,61	0,99	0,17	2,21	15,08	0,54	0,71	-0,13
BBP33	12,02	17,07	7,80	1,89	0,59	1,61	0,60	0,59	0,55	0,73	0,01	10,52	43,46	9,63	1,42	0,31	0,24	2,69	16,47	0,32	0,76	-0,16
BDK20	10,68	8,01	4,95	0,78	0,82	0,55	0,33	0,62	0,65	0,78	0,03	4,01	28,92	8,53	1,78	1,05	0,16	3,11	13,69	1,02	0,46	0,41
BDK21	10,61	11,68	0,79	1,67	0,88	1,80	0,66	1,82	0,56	0,52	0,08	4,89	29,4	5,77	1,10	0,53	2,11	2,79	20,40	0,40	0,95	-0,21
BDK26	14,35	16,96	9,01	2,60	0,46	1,51	0,68	0,48	0,56	0,34	0,05	5,05	47,0	11,98	1,18	0,18	0,29	5,60	42,20	0,25	0,64	-0,23
MIN.	5,01	6,22	0,79	0,67	0,32	0,45	0,33	0,40	0,52	0,32	0,02	2,80	17,34	5,77	0,36	0,18	0,16	1,30	6,49	0,20	0,25	-0,73
MAX.	43,33	48,65	23,53	5,59	4,40	5,50	2,33	3,99	3,32	3,44	0,47	43,44	150,11	13,85	2,09	1,03	2,11	3,28	46,01	1,02	0,95	-0,02
Mean	17,64	22,68	11,36	2,85	1,90	2,00	0,84	1,73	1,43	1,36	0,16	14,84	64,15	8,09	1,88	0,67	0,33	2,77	16,41	0,51	0,72	-0,16

ΣCe/ΣY=(La+Ce+Pr+Nd+Sm+Eu)/(Gd+Th+Dy+Ho+Er+Tm+Yb+Lu+Y); LEER/HREE=(La+Ce+Pr+Nd+Sm+Eu)/(Gd+Tb+Dy+Ho+Er+Tm+Yb+Lu); Eu/Eu\*=[Eu<sub>157</sub>]/(Sm<sub>147</sub>XGd<sub>157</sub>)<sup>1/2</sup>; Ce/Ce\*=[Ce<sub>135</sub>]/(La<sub>138</sub>+Nd<sub>142</sub>)<sup>0,31</sup>; Ce<sub>anom</sub>=shale-normalised<sup>(15)</sup> [2Ce/(La+Pr)]; Ce<sub>anom</sub>=Log[3Ce<sub>N</sub>/(2La<sub>N</sub>+Nd<sub>N</sub>)]<sup>(10,18)</sup>. The subscript "N" and "SN" indicate chondrite-normalized values and shale-normalized values, respectively. BOP: Oolitic/pisolitic ore, BM: Massive ore, BD: Detritus-rich ore, BBP: Broken pisolitic ore, BYK: Wallrock samples.

Table 3: Rare earth element analyses of the ore samples and wallrock from the Binkılıç Mn deposit (ppm).

5,38 to 58,31 showing a dominance of Mn over Fe. The average Mn/Fe ratios in oolitic/pisolitic ore and massive ore are 21,20 in seven samples and 20,98 in four samples, respectively. Other types of ores include lower Mn/Fe ratios (for detritus-rich ore 7,90, for broken pisolitic ore 13,91). Comparing the geochemical data of various Mn deposits [8,15-19] revealed that the Binkılıç Mn deposit contain lower Mn/Fe ratios than those of hydrothermal, and sedimentary exhalative deposits and are similar to those found in basin margin shallow-water sediments with contribution of fresh water.

Geochemical data of manganese deposits have been used in some discrimination diagrams that indicate a sedimentation environment and genetic origin. The Na-Mg discrimination diagram (Figure 3) allows us to understand the relationships between Mn oxides deposited in the fresh water, shallow-marine and marine environments. In this diagram, most of the Binkılıç samples fall in the area that represent shallow marine depositional environment, while some samples indicate a fresh water environment. In Figure 4, data from the Binkılıç Mn deposit plot in the fields of a hydrogenous origin due to their low silica values. Roy [17] suggested that hydrothermal deposits commonly occur in close association with the ferruginous silica gel formed by submarine effusive processes and metal discharge into marine sediments

At Binkılıç, the carbonate content of the manganese ore body is higher than other similar sedimentary deposits such as Chiatura and Nikopol [3,4]. The CaO values of the deposit vary from 6,74 to 46,60%, with an average value of 24,59% (Table 1). According to correlation data [8], the Ca shows poor and intermediate correlation coefficients (Mn:  $r=-0.576$ , Fe:  $r=0.011$ , Si:  $r=-0.061$ , Al:  $r=-0.179$ ). These weak correlations values suggest that the precipitation of carbonated material

was dominant in the formation of Mn deposit in Binkılıç and controlled the carbonate and manganese mineral assemblage. The Al is generally associated with clay minerals in this type of deposits, and possess much better values when correlated to Ti ( $r=0.886$ ). The average  $TiO_2$  value in the Binkılıç deposit is about 0,60%. The relatively high Ti values in Mn deposits are a reflection of some mixing of detrital material during precipitation, producing an extremely good correlation between Al and Ti [8,14].

The trace elements of the Binkılıç Mn deposit varies in a wide range (Table 2). and not reflect a significant difference among the ore types. Nevertheless, some trace element contents (such as Ba, Co, Sr, Cu, Zn and Ni), in general, are higher in the Oolitic/pisolitic and massive ore and show the positive correlation with manganese. The concentration of these elements is closely related to the increase of manganese content and indicate the element's nature in various manganese minerals. In the formation of Mn deposits, some trace elements such as Ni, Pb and Zn that may form isomorphous compounds could form oxides with manganese by oxidizing environment's effect. At last, they cause the formation of formative oxides such as  $Zn_2Mn_3O_3$ ,  $Ni_2Mn_3O_8$  and  $Pb_2Mn_3O_8$  that contain Mn in more oxidized form. Thus, Ni, Pb and Zn are accordingly enriched along with Mn elementary ceaseless concentration [20].

Co, Cu, Zn and Ni contents of Mn-oxides, especially Co/Ni and Co/Zn ratio, have been used in various discrimination diagram for the depositional environment. As well known, behavior of Co closely follows Ni. Co and Ni concentration ranges in the Binkılıç Mn orebody are 15 ppm-149 ppm and 27 ppm-350 ppm, respectively (Table 2). Co and Ni reach their highest concentrations in the oolitic/pisolitic ore. The Co/

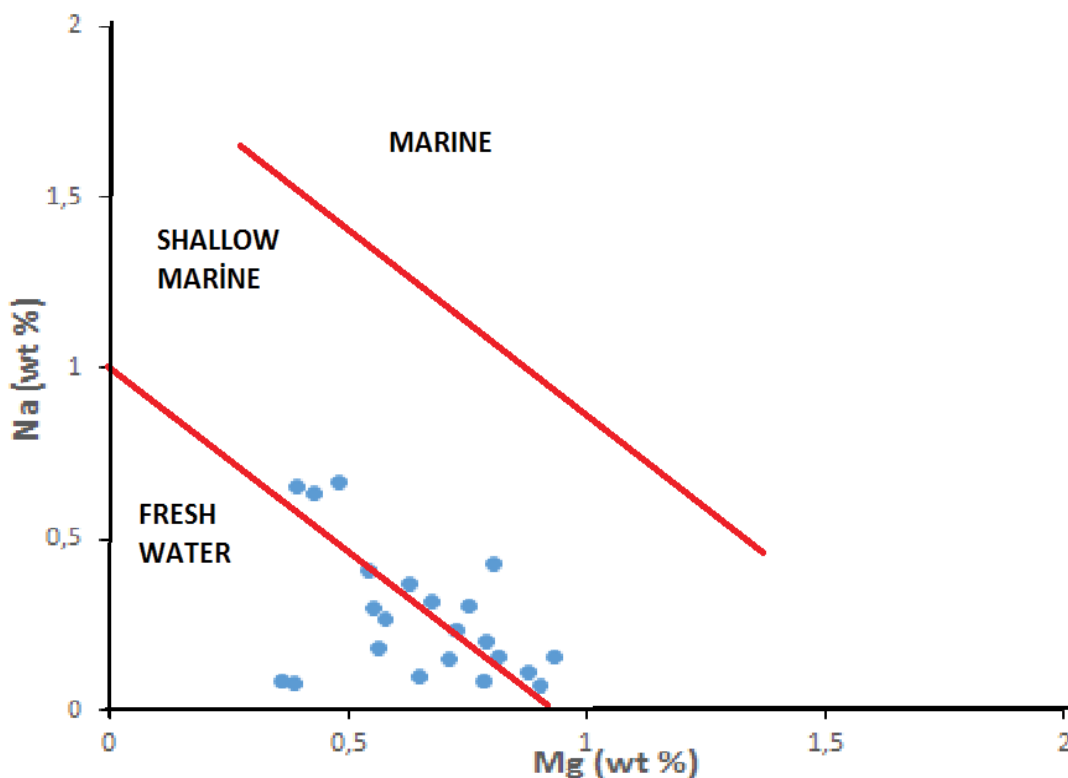


Figure 3. Diagnostic plot to differentiate marine and fresh water deposits (Nicholson, 1992). The samples from Binkılıç mine share the shallow and fresh water fields.

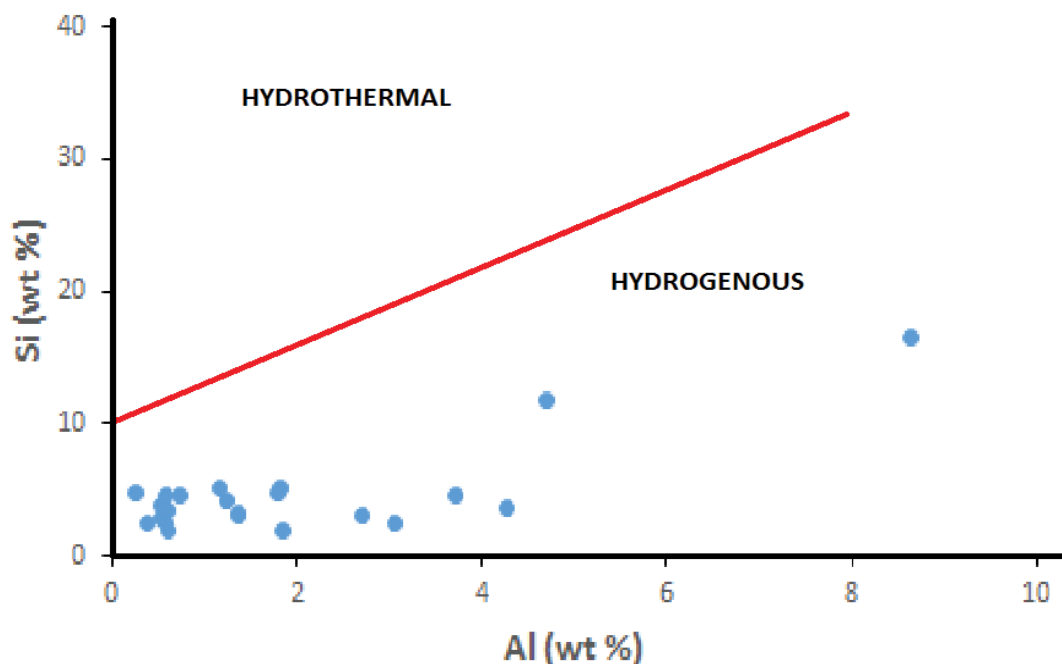


Figure 4: Al-Si discrimination diagram for the Binkılıç samples (Choi and Hariya, 1992). All of the samples plot in the hydrogenous field.

Ni ratio of the ore varies between 0,18 and 1,27, with an average value of 0,73. According to some researchers [16,21-23] Co / Ni ratio can be used as a criterion in the determination of depositional environments, particularly hot water sedimentation on the sea floor. In general, the samples from hydrogenous Mn deposits show a strong positive Co anomaly. Although Cu, Ni and Zn are related to hydrothermal deposits in origin, hydrothermal oxides are depleted in Cu, Ni and Co relative to hydrogenous deposits [24].  $Co/Ni < 1$  is indicative of sedimentary origin while  $Co/Ni > 1$  represents for a deep marine environment [16]. These ratios in the Binkılıç ore samples are lower than 1 in 18 samples. The ratios of greater than 1 are determined only in total 2 ore samples belong to detritus-rich ore and broken pisolitic ore. In general,  $Co/Zn$  ratio of 0,15 is indicative of hydrothermal type deposit and a ratio of 2,5 indicates hydrogenous type deposits [15,18]. This ratio (average 1,34 ppm) for the Binkılıç Mn deposit are found to be greater than 0,15 (Table 2). The  $Co/Ni$  and  $Co/Zn$  ratios show that the depositional environment at Binkılıç is a hydrogenous character.

The Binkılıç Mn ores are also characterized by high average contents of Ba (average 2125 ppm) and Sr (average 2664 ppm). Interestingly, the ore shows low V concentrations with an average value of 39,82 ppm, whereas other Mn deposits such as Chiatura and Nikopol that formed in shallow marine environments contain higher V concentrations [16].

In manganese deposits, some discrimination diagrams provide important evidences to determine their origin. In Mn-Fe-(Co+Ni+Cu)×10 triangular diagram, all samples are plotted in both hydrogenous and diagenetic fields (Figure 5a). In general, a scattering is observed in (Figures 5b and 5c). In Figure 5b, the samples indicate a trend towards the diagenetic field from the hydrothermal area. In the Ni-Zn-Co diagram, some samples indicate the hydrogenous field, but others are plotted outside the descriptive fields (Figure 5c). The results reflect interaction of many elements. Although, some element contents

show a low concentration, they can play an important role in manganic concentration process.

Trace element spider diagram normalized to shale composite NA is given Figure 6. In this diagram, variation curve features of all the ore types and wallrock seem to be consistent with each other. They are clearly enriched in Sr, Ni while distinctly depleted in Rb. The Co content of the samples shows slightly an enrichment. Sr concentration in the oolitic/pisolitic and massive ore is richer than those of the detritus-rich and broken pisolitic ore. Consistent with this depleted trend, Cr also showed depletion. The similarities observed in spider curves of ore samples indicated that the origin of material and ore-forming conditions is similar. Thus, ore-forming material possibly went through different differentiation and evolution under same resource condition. From the geochemical data of trace element, it can be said that trace elements in the oolitic/pisolitic and massive ores are more concentrative in oxidizing process of manganese ore [15]. On the other hand, all the data show that sedimentary water body during the formation of detritus ore might be deeper than that of the oolitic/pisolitic and massive ore.

#### Rare earth elements (REE) characteristics

The REE results of Binkılıç samples are listed in Table 3. The total REE contents of the ore samples vary from 17,34 ppm to 150,11 ppm, averaging 64,15 ppm and can be compared to the average of the sedimentary rocks of Eugeosyncline zones. The  $\Sigma REE$  in these types of sedimentary rocks is from 30 ppm -127 ppm, with an average 103 ppm and belong to LREE-enriched type. The average REE contents in the carbonates associated with Eugeosyncline zone vary between 30 ppm and 47 ppm, while the clays have a uniformly high 'platform-like' REE concentrations [25]. At Binkılıç, the carbonates are wallrock for the manganese ores and all the ore samples contain significant carbonate minerals, especially in oolitic and pisolitic form. The similarity of REE

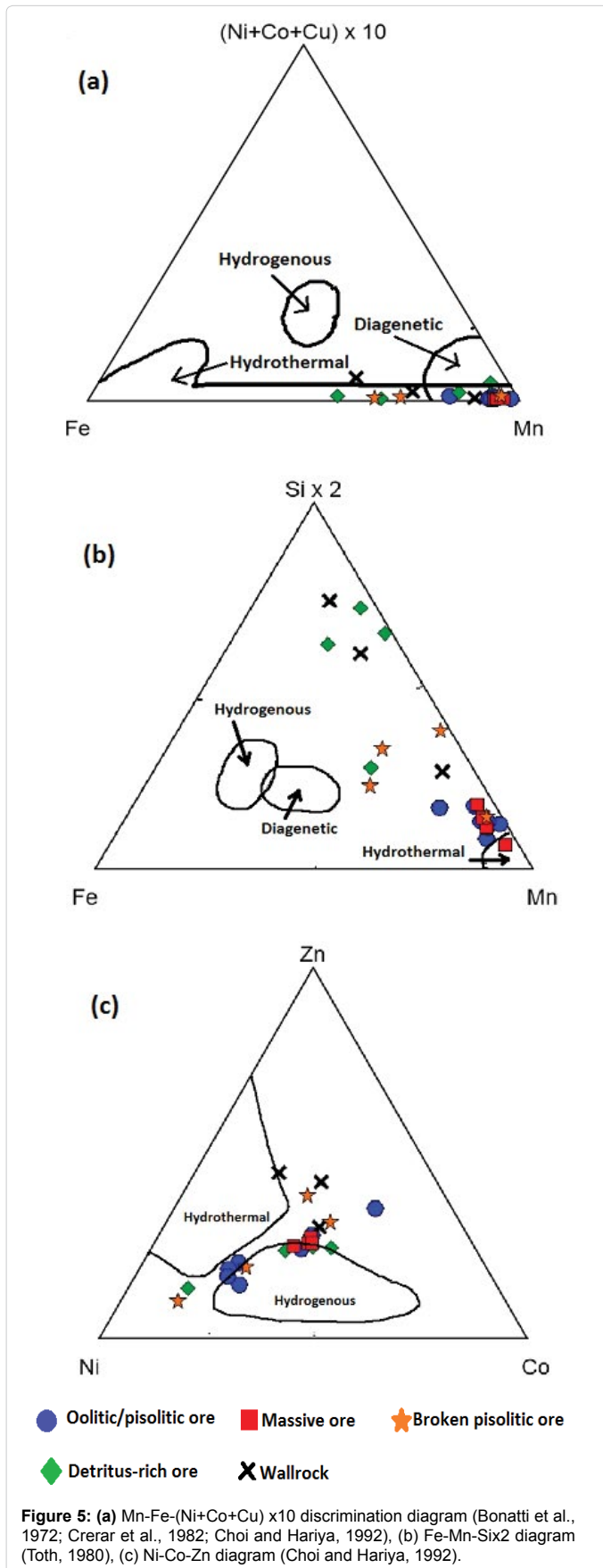


**Figure 5:** (a) Mn-Fe-(Ni+Co+Cu) x10 discrimination diagram (Bonatti et al., 1972; Crerar et al., 1982; Choi and Hariya, 1992). (b) Fe-Mn-Si x 2 diagram (Toth, 1980). (c) Ni-Co-Zn diagram (Choi and Hariya, 1992).

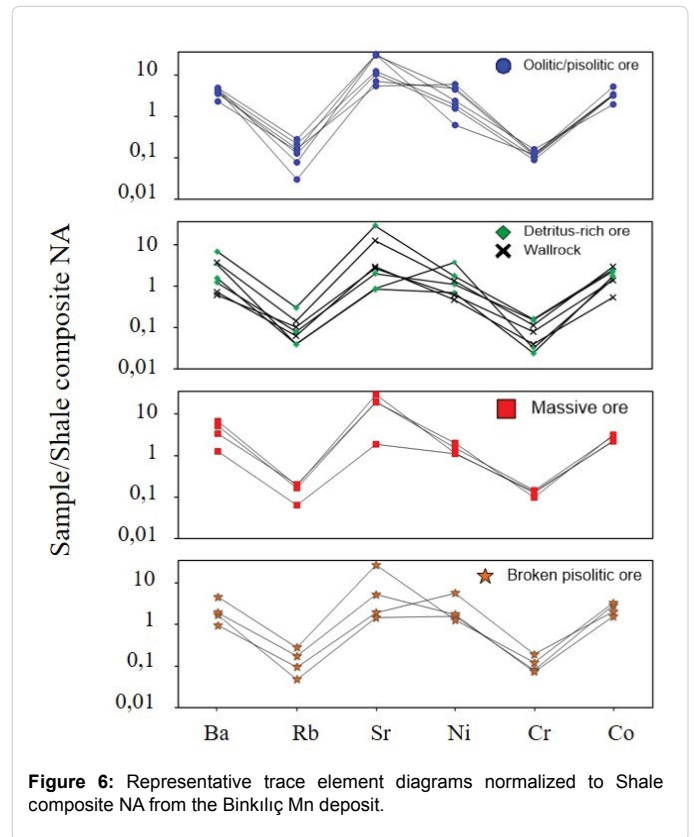


**Figure 6:** Representative trace element diagrams normalized to Shale composite NA from the Binkılıç Mn deposit.

contents in both ore samples and wallrock indicates the same source for these elements. When the only ore samples are taken into account, REE contents of the detritus-rich ore samples are lower than those of the other type ores. Because more carbonate minerals were developed during the formation of detritus-rich orebody and the ore-forming solutions have higher  $\text{CO}_3^{2-}$  contents, REE possibly as complex Mn-carbonate compounds were removed by solutions, causing total REE to fall. However, all ore types have the same variation tendency (Table 3), normal tendency of REE concentration to increase towards the massive oxide ore was accentuated by enrichment during oxidative concentration process of manganese deposit.

Total light REE /heavy REE ( $\Sigma\text{LREE}/\Sigma\text{HREE}$ ) and Ce/La ratios can be used an indicator of prior enrichment in the forming process of Mn deposits. At Binkılıç, the ratio of  $\Sigma\text{LREE}/\Sigma\text{HREE}$  varies between 5,77 and 13,85 (average 8,09, Table 3). These values indicate that a primary enrichment for LREE has occurred in Binkılıç Mn oxidation process. Generally,  $\text{LREE} > \text{HREE}$  may be an indicator for hydrothermal Mn deposits and LREE's are supplies by volcano clastics while HREE's are from  $\text{MnO}_2$  that is precipitated in seawater. However, increase in total LREE may be associated with the amount of terrigenous material that was transported in the depositional environment. In such a case, manganese and total HREE show decreasing trends.

The Ce/La ratios of Binkılıç Mn deposit vary from 0,36 to 2,09 with an average 1,88. This ratio shows a similarity for the orebody and wallrock and are good indicator for the degree of Ce depletion in sediments [26]. Hydrogenous iron and manganese deposits indicate low Ce/La ratio (~0,12), while the deposit with carbonaceous biogenic and terrigenous material addition have higher Ce/La ratio. According to Dubinin and Volkov [27] this value could be 3 or more for some

rocks (ore) types in the Mn-bearing sequence. Ce/La ratios of Binkılıç ore were accentuated by increasing terrigenous materials in the depositional environment (Table 3).

The relationship between manganese deposits and their REE contents has been studied by various researchers. In all these studies, there is no generally accepted model for reflecting the deposit type and oxidative and reductive depositional conditions [26]. In addition to Ce and Eu, the ratios of  $\Sigma Ce/\Sigma Y$ , Eu/Sm, Sm/Nd belonging to the orebody and wallrock are commonly used for the prediction of fluid source and redox potential of the environment. These ratios in a manganese sequence are comparable to those of rocks from the continental and subcontinental crust, but differ from those of the oceanic crust [15]. The different sources of sediment matter may affect the distribution of REE in sediment. According to the Ranov [25], the crystalline basement of the Russian platform contains a relatively light REE composition ( $\Sigma Ce/\Sigma Y=3,2$ ) and the ratio of Eu/Sm of the platform is 0,26. The sedimentary cover of the platform inherits this REE distribution almost without change ( $\Sigma Ce/\Sigma Y=3,4$ ), Eu/Sm=0,21). The trend of the REE distribution is slightly different for volcanic rocks and the increase in their concentration causes the systematic changes in REE composition. Light lanthanides increase ( $\Sigma Ce/\Sigma Y$ ) varies from 1,4 to 7,5 and the value of the Eu/Sm ratio decreases from 0,31 to 0,21. At Binkılıç, the ratios of the  $\Sigma Ce/\Sigma Y$  and Eu/Sm vary from 1,30 to 3,28 with the mean value of 2,77 and from 0,18 to 1,03 with the mean value of 0,67 respectively (Table 3). Consequently, the value of  $\Sigma Ce/\Sigma Y$  ratio of the samples from Binkılıç Mn deposit is similar to those of the Mesocenozoic carbonates, with a mean values of 2,70 [25], but the values of Eu/Sm ratio distinctly high, indicating the influence of different sources of sediment matter.

At Binkılıç, the manganese occurrences associated with the sedimentary rocks, especially carbonates seem to be distinctive. When  $Eu^{3+}$  and  $Eu^{2+}$  co-existed in solution of Ca-bearing carbonate,  $Eu^{3+}$  prior to  $Eu^{2+}$  substituted for  $Ca^{2+}$  to enter into carbonate, and was removed by solutions [16,28]. Therefore, the native manganese carbonate ores mostly show a large Eu depletion based on this elemental substitution. In the Binkılıç Mn deposit, the Eu anomaly was computed with the formula of  $Eu/Eu^* = [(Eu)/(Sm \times GdN)]^{1/2}$ , where  $Eu^*$  is the hypothetical concentration [26]. A middling positive Eu anomaly is observed in all ore samples from the Binkılıç orebody and the  $Eu/Eu^*$

anomaly values range from 0,20 to 1,02 with an average 0,51 (Table 3). We conclude that a positive Eu anomaly reflects an interaction of ground water with substrata volcanic rocks and the absence of any contamination from the continental crust.

The normalized REE patterns in Figure 7 indicate relatively similar distribution characteristics and may point similar depositional environment and condition. These patterns of the Binkılıç samples are compatible with those of hydrogenous Mn deposits. In general, the hydrothermal Fe-Mn deposits demonstrate the different distribution patterns. The results of geochemical studies show that hydrogenous Mn deposits are more enriched in REEs than their hydrothermal equivalents.

Differences in REE relative fractionations and total abundances in sedimentary rocks reflect the depositional location of the sediments [15,29-34]. So, the Ce' anomaly in the sedimentary rocks play an important role as indicators of certain tectonic environment. The shale-normalized Ce' anomaly and total REE abundance ( $\Sigma REE$ ) variations generally preserved in deep sea sediments due to stable characteristics of REE in different geologic process. The studies have revealed that the formed Ce' anomaly is not affected by the late period geologic process. According to Murray [32], the sedimentary rocks near the spreading ridge under the influence of metalliferous activity are characterized by extremely low Ce anomalies ( $Ce^* = \text{about } 0.29$ ). The same rocks from an ocean-basin floor and from continental margin region have less extreme Ce anomalies, with  $Ce^*$  values of about 0.55 and slight  $Ce^*$  anomalies ranging from 0.90 to 1.30, respectively. These result show that the manganese deposit in the Binkılıç district are mainly associated with the marine basin ( $Ce^*$  anomaly  $> 0.90$  in 17 samples).

### Depositional conditions of rare earth elements

The REE mixing or evolution trends in the deposits should be produced by some differences in elemental composition of depositional environment. Figure 8 contain NASC (North American Shale Composite)-normalized values of Yb (HREE), Gd (MREE) and Nd (LREE) in the Binkılıç samples. The ore samples roughly plot along a line, which reflect a similar trend (from high YbN content to high GdN and NdN contents). This may result from mixing or evolution between two end member waters, one enriched in MREE and LREE, and the

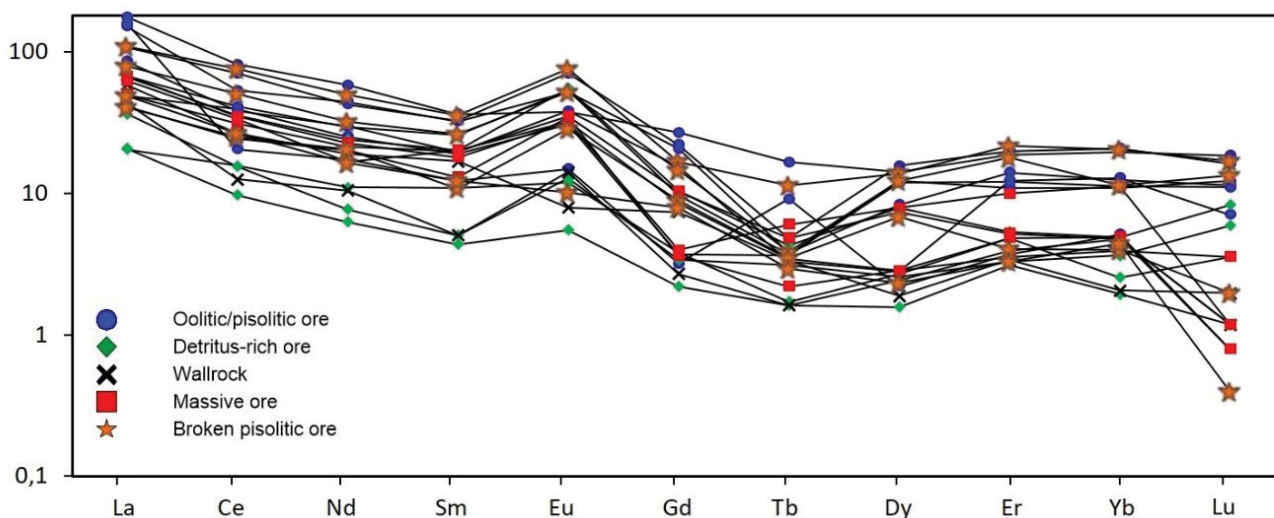
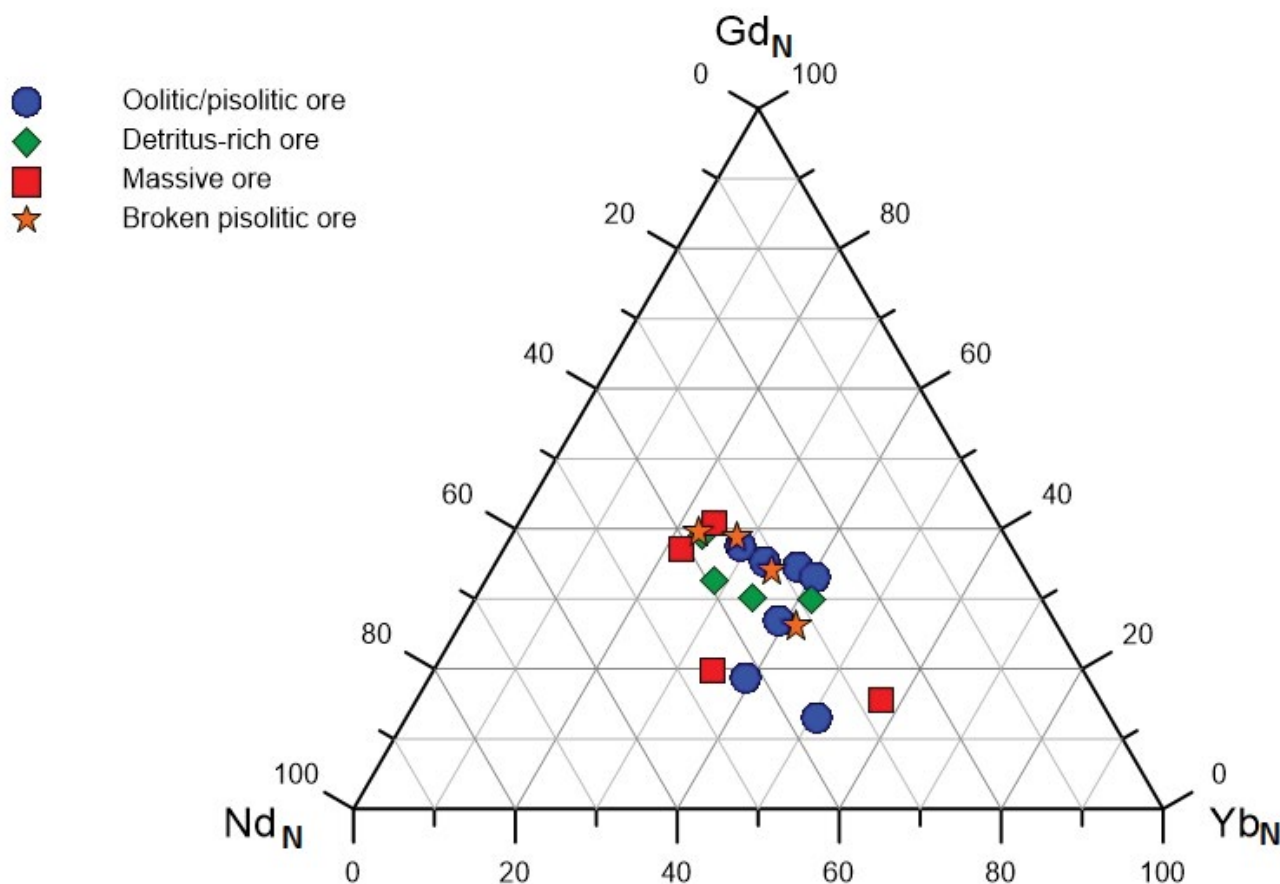


Figure 7: Chondrite-normalized REE patterns of ore and rock samples from manganese deposit (Normalization values are from Evensen et al., 1978).



**Figure 8:** Ternary diagram of shale-normalized values of Yb (HREE), Gd (MREE) and Nd (LREE) in ore samples from Binkılıç deposit. Normalization values (North American Shale composite, NASC) are from Groment.

other enriched in HREE. In a sedimentary environment, the REE content of bottom waters may be significantly modified by any upward flux of REE from the sediment water interface or sediment pore. Differences in REE signatures in the ore samples could be explained by mixing between LREE-MREE-enriched anoxic water (or fresh water) and HREE-enriched oxic open marine water [30].

The patterns of chondrite-normalized REEs of the Binkılıç samples are remarkably similar, yielding HREE-depleted curves with a small negative Ce and middle positive Eu anomalies (Figure 7). Also, the shale-normalized REE patterns of the Mn-bearing sequence's samples from the Thrace basin are similar, yielding and nearly regular patterns with smaller negative anomalies for Ce [16]. The strong positive Eu anomalies reflect the oxidizing sedimentary environment, but the meaning of point-facies of Gd is still unknown. Oxidation-reduction potential in sedimentary environments markedly affects the Ce content. When the oxidation zones are enriched in Ce, the oxide ores are of high Ce content. In briny pH and Eh condition, Ce is oxidized to  $Ce^{4+}$ , its solubility is very small, and thus it is not easy to stay in sea water, so host rocks or ore show relatively Ce depletion. The published data from manganese deposits [9,18-20,25-27,35] show that hydrogenous manganese deposit contain positive Ce anomaly, while hydrothermal deposits are characterized by negative Ce anomalies. In the other hand, negative Ce anomalies together with HREE enrichments are strong indicator of an oxic depositional environment and attributed to open

ocean environment, while positive Ce anomaly together with LREE-to MREE-enriched profiles indicate anoxic conditions [35]. The ratios of  $Ce/Ce^*$  in Binkılıç Mn deposit range from 0,25 to 0,95, with an average of 0,72 (Table 3). Although, these values together with negative Ce anomaly show mainly an oxic depositional environment, it can be said that sometimes the anoxic conditions are effective in the depositional environment.

The relationship among Ce, La and Nd of REE could be explained as Ce anomaly ( $Ce_{anom}$ ), calculative formula of  $Ce_{anom} = \log[3 \times Ce_N / (2 \times La_N + Nd_N)]$ . The subscript N indicates shale-normalized value from McLennan [35]. The values of the Binkılıç samples vary from -0,73 to -0,02. The values of  $Ce_{anom} > -0,1$  may represent enrichment of  $Ce_{anom}$  and reflect the sedimentary water body in oxygen-lack environment. The values of  $Ce_{anom} < -0,1$  may represent negative anomaly Ce and reflect the sedimentary water body in oxidative environment. Ce anomalies in the Binkılıç Mn deposit were found as  $Ce_{anom} < -0,1$  in 19 samples and  $Ce_{anom} > -0,1$  in only 3 samples. These results indicate both anoxic and oxic conditions for the depositional environment.

## Discussion

The Binkılıç Mn deposit was taken place within the Oligocene fossiliferous formations of a Tertiary collisional-collapse type basin. There is no doubt that the Binkılıç Mn deposit is originally a sediment-

type deposit. The compositional trends and geologic evidence [5,8,12,14,17] indicate that relatively rapid marine transgressive-regressive events which caused the sea-level changes are effective on the mineralization process. Despite the strong sedimentation data, hydrothermal input to depositional environment is not clear enough. Furthermore, geochemical data indicate that a hydrothermal contribution is negligible or weak. Thus, we consider that the main elementary source especially for manganese is runoff and fluvial sediment loads from the metamorphic rocks of the Stranjha Massif, as well as dissolved Mn-bearing groundwater derived from the same rocks [36]. As a result of these, it can say that the marine environment and pore water primarily is enriched in dissolved  $Mn^{2+}$ .

At Binkılıç, manganese oxides with variable carbonate content constitute the predominant ores. The fine laminations, oolitic and pisolitic textures seem to be as characteristics of the sedimentary deposition in a marine environment. Some different processes have been proposed for the formation of Mn oxides. Some researches [8,14] suggest that the Mn oxides formed by upwelling of reducing waters containing abundant organic matter and dissolved Mn to the shallow-marine areas but the other studies [5,12] suggested that the deposit formed from groundwater which infiltrated and replaced the original calcitic material of the Congeria Series with Mn Carbonates. These interpretations emphasize an interaction between marine pore water and groundwater.

Nicholson [24] summarized positive correlations of elements with manganese in different genetic types of deposit. Despite some recognized limitation, three correlations are identified as potentially diagnostic, namely Mn-Ba for fresh water oxides; Mn-Pb for dubhites (oxides formed by the weathering of a mineralized sequence), and Mn - As for hydrothermal deposits. According to the author, geochemical associations are related to a given deposit type and normalization of the oxide chemistry against manganese content can be employed as a discriminatory in defining element pattern. At Binkılıç, the following significant geochemical association has been shown in the majority of analyses: Mn-Ba-Sr-Co-Cu-Ni. This geochemical association, i.e. the positive correlations of elements with manganese displays a marked element enrichment in the deposit and are similar to diagenetic Mn deposits formed in the marine environments [16]. In general, diagenetic processes cause the enrichment of Mn, Cu, Ni and the trace elements in the manganese deposits. The enrichment of trace elements could be related to adsorption from pore water [16,17,20,24].

The Mn/Fe ratios of sedimentary Mn deposit are generally less than those of volcano-sedimentary occurrences. Data from Hazara-Pakistan [19] and Ulukent-Turkey [7] deposit are compatible with those of sedimentary deposit in marine environment. The average Mn/Fe ratios of both deposits are 2,16 and 18,98, respectively. This ratio in the Eymir manganese deposit, an exhalative sedimentary deposit is raise to 880,33 [10]. At Binkılıç, the Mn/Fe ratios are in the range of 1,38 and 58,31, with an average of 16,76 (Table 1).

Jian cheng [20] consider that Co/Ni ratio is a good indicator that judges the sedimentary environment and sedimentation, which is especially a hot water sedimentation of sea bed. The Co/Ni values of the Binkılıç deposit are in the range of 0,18-1,27 (average=0,73). The ratios of the ore samples, except for the samples BD28, is lower than 1, similar to sedimentary manganese deposits. However, the values indicate that the sedimentation in the Binkılıç district is not represent a hot water sedimentation.

Other discriminative parameters for Binkılıç Mn deposit are the

Ba and Sr contents and the Sr/Ba ratio. The barium and strontium concentrations show differences in the ore and wallrock samples, ranging from 450 to 4320 and from 210 to 5980 respectively (Table 2). Sr/Ba ratios in the ore samples are greater than 1 in 9 samples, but lower than 1 in 10 samples. In general, in fresh water sedimentation  $Sr/Ba < 1$ , but in marine deposit  $Sr/Ba > 1$ . The variable Sr/Ba values indicate that the Mn oxide ores are associated with both the marine sedimentary environment and fresh water sedimentation, but the samples of the wallrock is greater than one, which can distinctly reflect the Sr enrichment in Mn-bearing carbonates. High Ba content of the Binkılıç Mn deposit is also indicative of sedimentary origin.

## Conclusion

The Binkılıç ore deposit evolved as consequences of various different interplays. From major oxide, trace element and REE assessments, we concluded that the Binkılıç Mn deposit occurred in a sedimentary environment and not contain any hydrothermal activity. The abundance of oolitic and pisolitic carbonate, mineral paragenesis, dissolution of calcite pisolites and diagenetic alteration from primer calcite to Mn carbonate and Mn oxide indicate a diagenetic type of Mn deposit with terrigenous material addition. The dissolved Mn-bearing groundwater is possibly interacted with marine porewater of carbonates which is relatively enriched Mn and other metals, thus both together were responsible for mineralization. However, we suggest that some Mn oxides formed by upwelling of reducing waters containing abundant organic matter and dissolved Mn to the shallow-marine areas containing oxidic conditions. This deposition may represent the first mineralization subsequently affected by diagenetic alteration. The proposed mineralization model here is different from the other Oligocene manganese deposits, such as Chiatura and Nikopol deposits originated from shallow marine environment. The discrimination diagrams presented in this paper also supported this type of model.

## References

1. Gültekin AH (1997) Mineralogical and chemical doses are used to determine the origins of manganese deposits. Geol Eng 50: 39-46.
2. Öztürk H (1993) Turkey matakana manganese formations and types. Geol Eng 43: 24-34.
3. Varentsov IM, Rakhmanov VP (1980) Manganese deposits of the USSR (A review). Geol & Geochem Mang. 2: 319-391. Bolton
4. Bolton BR, Frakes LA (1985) Geology and genesis of manganese oolite, Chiatura, Georgia, U.S.S.R. Geol Soc Am Bull 96: 1398-1406.
5. Öztürk H, Frakes L (1995) Sedimentation and diagenesis of an Oligocene manganese deposit in a shallow sub-basin of the paratethys: Thrace Basin, Turkey. Ore Geol Rev 10: 117-132.
6. Gedikoğlu A, Van A, Eyüpoğlu I, Yalçın B (1985) An example of the mineralization of the eastern Black Sea is: Manganese in January (Maçka). Geol Eng 25: 23-35.
7. Kuşçu M, Gedikoglu A (1989) Geochemical Properties of Manganese deposits in Ulukent (Tavas - Denizli) South. Terrestrial 17: 29-41.
8. Gültekin AH (1998) Geochemistry and origin of the Oligocene Binkılıç manganese deposit, Thrace basin, Turkey. Tr J Ear Sci. 7: 11-23.
9. Gültekin AH, Balcı N (2016) Mineralogy, geochemistry and fluid inclusion data from the Tumanpınarı volcanic-hosted Fe-Mn-Ba Deposit, Balıkesir-Dursunbey, Turkey. Minerals 6: 1-26.
10. Oksuz N (2011) Geochemical characteristics of the Eymir (Sorgun-Yozgat) manganese deposit, Turkey. J Rare Earths 29: 287-296.
11. Akartuna M (1953) Çatalca-Karacakoy region geology. Istanbul University Monograph 3: 80.
12. Bora E (1969) The geology and Mn mineralizations of the Binkilic and Sefaaalan area. Unpublished MSc thesis, Univ Istanbul 47.

13. Uzkut I (1971) Turkey madencilg manganese and future. MTA Dergisi 77.
14. Gokcen N (1973) The age and the lateral facies changes of the Pinarhisar Formation (Oligocene), NE Thrace. Mineral Res-Explor Bull Turkey 113: 15-29.
15. Rona PA (1978) Criteria for recognition of Hydrothermal Mineral Deposits in Oceanic crust. Econ Geol 73: 135-160.
16. Choi JH, Hariya Y (1992) Geochemistry and depositional environment of Mn oxide deposits in the Tokoro Belt, Northeastern Hokkaido, Japan. Econ Geol 87: 12-65.
17. Roy S (1992) Environments and processes of manganese of manganese deposition. Econ Geol 87: 1213-1236.
18. Fitzgerald CE, Gillis KM (2006) Hydrothermal manganese oxide from Baby Bare seamount in the Northeast Pacific Ocean. Marine Geol 225: 145-156.
19. Shah MT, Moon CJ (2007) Manganese and ferromanganese ores from different tectonic settings in the NW Himalayas, Pakistan. J Asian Earth Sci 29: 455-467.
20. Jian cheng X, Xiaoyong Y, Jiongo D, Wei X (2006) Geochemical characteristics of sedimentary manganese deposit of Guichi, Anhui Province, China. J Rare Earths 24: 374-380.
21. Bonatti E, Kraemer T, Rydel H (1972) Classification and genesis of submarine iron-manganese deposits. Natl Sci Found 149.
22. Crerar DA, Namson J, Chyi MS, Williams L, Feigenson MD, et al. (1982) Manganiferous cherts of the Franciscan Assemblage: I. General geology, ancient and modern analogues and implications for hydrothermal convection at oceanic spreading centers. Econ Geol 77: 5-19.
23. Hein JR, Bolton BR (1992) Stable isotope composition of Nikopol and Chiatura manganese ores: Implications for genesis of large sedimentary manganese deposits. 29th Int Geol Congr Kyoto1: 209.
24. Nicholson K (1992) Contrasting mineralogical - geochemical signatures of manganese oxides: Genesis to metallogenesis. Econ Geol 87: 1253-1264.
25. Ranov PA, Balashov YA, Girin YP, Bratishko RKN, Kazakov GA, et al. (1974) Regularities of the rare-earth element distribution in the sedimentary shell and in the crust of the earth. Sedimentol 21: 171-193.
26. Kahrazezi M, Lotfi M, Ghaderi M, Mohajjel M, Jafari, M, et al. (2015) First report of geochemical characteristics of the Sangam manganese occurrence, Northeast Khash (Iran). Ind J Sci & Technol 8: 85-93.
27. Dubinin AV, Volkov II (1986) Rare earth elements in metalliferous sediments of the East Pacific rise. Geokhimiya 5: 645.
28. Lee JH, Byrne RH (1993) Complexation of trivalent rare earth elements (Ce, Eu, Gd, Tb, Yb) by carbonate ions. Geochim Cosmochim Acta 57: 295-305.
29. Evensen MN, Hamilton PO, Nions RK (1978) Rare-earth abundances in chondritic meteorites. Geochem. Cosmochim Acta 42: 1199.
30. Wright J, Schrandt H, Holser WH (1987) Paleoredox variations in ancient oceans recorded by rare earth elements in fossil apatite. Geochimica et Cosmochimica Acta 15: 631-644.
31. Peters T (1988) Geochemistry of manganese-bearing cherts associated with Alpine-ophiolites and the Hawasina formations in Oman. Marine Geol 84: 229-237.
32. Murray RW, Buchholtz Ten Brink MR, Jones DL (1990) Rare earth elements as indicators of different marine depositional environments in chert and shale. Geol 18: 268-271.
33. David ZP, Bau M (2013) Normalized rare earth elements in water, sediments, and wine: Identifying and environmental redox conditions. Am J Anal Chem 4: 69-83.
34. Fadela A, Zigaite Z, Bloma H, Perez-Huertac A, Jeffries T, et al. (2015) Palaeoenvironmental signatures revealed from rare earth element (REE) compositions of vertebrate micro remains of the Vesak Bone Bed (Homeric, Wenlock), Saaremaa Island, Estonia. Estonian J Earth Sci 64: 1-3641.
35. McLennan SM (1989) Rare earth element in sedimentary rocks: Influence of provenance and sedimentary processes. Rev in Mineral 21: 169-200.
36. Erarslan C, Orgün Y (2017) Mineralogical and geochemical characterization of the Saray and Pinarhisar coals, Northwest Thrace Basin, Turkey, Int J Coal Geol 173: 9-25.